Radiation Through an Inhomogeneous Reentry Plasma Layer

***Abstract*—The radiation from a TE excited slot antenna in a ground plane covered with an inhomogeneous plasma sheath is considered. The profile closely approximates that encountered in reentry situations and recently simulated in a laboratory plasma.**

In a recent paper, Stewart [1] reported the laboratory simulation of reentry plasma sheaths. The electron-density profiles of the laboratory plasmas were similar to those encountered in reentry situations [2]. Some radiation patterns of rectangular slot antennas in the presence of the inhomogeneous sheath have been calculated by Stewart and Golden [3], using a large number of homogeneous plasma slabs to model the sheath.

In this communication, the electron-density profile of the inhomogeneous plasma over a ground plane at $z = 0$ is modeled by a linearly increasing density, followed by an exponential decay. The plasma frequency is then given by

$$\omega_p(z) = \omega_{p0}\left(\frac{z}{z_0}\right)^{1/2}, \qquad 0 \le z \le z_0$$

$$= \omega_{p0} \exp\left(\frac{-(z - z_0)}{2z_1}\right), \qquad z \ge z_0. \tag{1}$$

ω_{p0} denotes the maximum value of plasma frequency, which occurs at $z = z_0$, and z_1 represents a measure of the thickness of the decaying portion of the profile. Collisions are neglected in what follows. The analytic form chosen for the electron-density profile is identical to that used by Stewart and Golden [3]. Because of the low collision frequency assumed, 1000 homogeneous slabs were needed to model the inhomogeneous plasma. For the electromagnetic field polarization and two-dimensional geometry assumed here, the boundary-value problem of a slot antenna in a ground plane covered with the inhomogeneous plasma sheath described by (1) may be solved in terms of known functions and the effect of the sheath calculated rather easily.

The geometry of the problem is shown in Fig. 1. At $z = 0$, the applied electric field is taken to be

$$\bar{E}(z = 0) = E_0(x)\bar{a}_y, \qquad |x| \le a$$

$$= 0, \qquad |x| > a. \tag{2}$$

The electromagnetic field is TE to the z direction and independent of y; the time dependence $\exp(-i\omega t)$ is assumed. The only electric field component present is E_y, satisfying

$$\frac{\partial^2 E_y}{\partial x^2} + \frac{\partial^2 E_y}{\partial z^2} + [k_0^2 - k_p^2(z)]E_y = 0 \tag{3}$$

subject to a radiation condition at infinity and the boundary condition of (2); $k_0^2 = \omega^2/c^2$ and $k_p^2(z) = \omega_p^2(z)/c^2$.

Upon taking Fourier transforms with respect to x, one finds that the transform of E_y may be expressed in terms of Airy functions in the region $0 \le z \le z_0$ and in terms of the modified Bessel function of the first kind of imaginary order when $z \ge z_0$. Solving the boundary-value problem in the usual way, one finds that E_y is given for $z \ge z_0$ by

$$E_y(x,z) = \int_{-\infty}^{\infty} F(h)Q(h,z) \exp(ihx) \exp[i(k_0^2 - h^2)^{1/2}z]\, dh \tag{4}$$

in which

$$F(h) = \frac{1}{2\pi}\int_{-a}^{a} E_0(x) \exp(-ihx)\, dx \tag{5}$$

Manuscript received January 29, 1971; revised April 19, 1971.

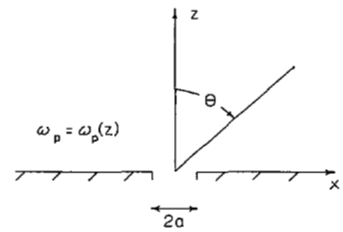

Fig. 1. Geometry of problem.

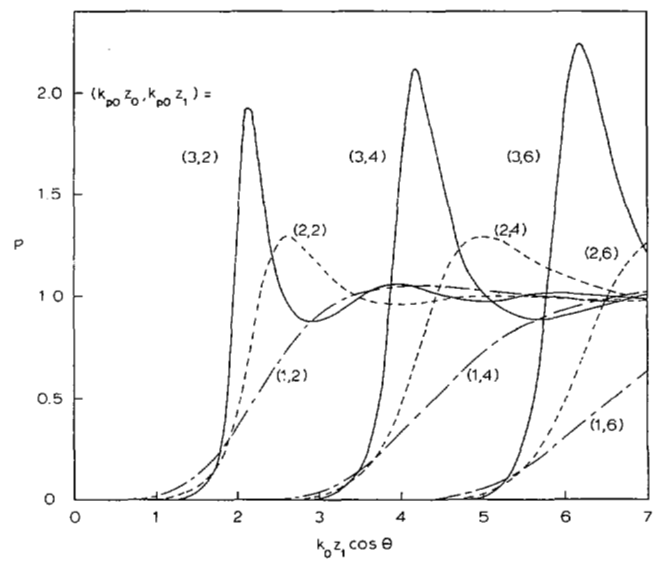

Fig. 2. Radiation pattern modification factors.

represents the transform of the applied electric field and

$$Q(h,z) = \frac{I_\nu(2k_{p0}z_1 \exp[-(z - z_0)/2z_1]) \exp[-i(k_0^2 - h^2)^{1/2} z]}{\pi I_\nu(2k_{p0}z_1)G_1 + \pi(k_{p0}z_0)^{1/3} I_\nu'(2k_{p0}z_1)G_2} \tag{6}$$

where

$$\nu = -2iz_1(k_0^2 - h^2)^{1/2}$$

$$G_1 = \mathrm{Ai}(\zeta_p)\,\mathrm{Bi}'(\zeta_0) - \mathrm{Ai}'(\zeta_0)\,\mathrm{Bi}(\zeta_p)$$

$$G_2 = \mathrm{Ai}(\zeta_p)\,\mathrm{Bi}(\zeta_0) - \mathrm{Ai}(\zeta_0)\,\mathrm{Bi}(\zeta_p)$$

$$\zeta_p = \frac{-z_0^{2/3}}{k_{p0}^{2/3}}(k_0^2 - h^2)$$

$$\zeta_0 = \zeta_p + (k_{p0}z_0)^{2/3}. \tag{7}$$

Ai(·) and Bi(·) denote, respectively, the Airy functions of the first and second kinds, and $I_\nu(\cdot)$ denotes the modified Bessel function of the first kind [4].

When z becomes large with respect to z_1, $Q(h,z)$ may be replaced by $Q(h,\infty)$:

$$Q(h,\infty) = \frac{(k_{p0}z_1)^\nu \exp[-i(k_0^2 - h^2)^{1/2}z_0]}{\pi\Gamma(1 + \nu)[I_\nu(2k_{p0}z_1)G_1 + (k_{p0}z_0)^{1/3} I_\nu'(2k_{p0}z_1)G_2]}$$

in which $\Gamma(\cdot)$ denotes the gamma function. The squared magnitude of $Q(h,\infty)$ is the factor by which the free-space radiation pattern is altered by the presence of the layer, when h is replaced by $k_0 \sin\theta$ [5]. $Q(k_0 \sin\theta, \infty)$ is a function of the three variables $k_{p0}z_0$, $k_{p0}z_1$, and $k_0 z_1 \cos\theta$. Curves illustrating $P \equiv |Q(k_0 \sin\theta, \infty)|^2$ as a function of $k_0 z_1 \cos\theta$ for various values of $k_{p0}z_0$ and $k_{p0}z_1$ are shown in Fig. 2.

Results for the case $k_{p0}z_0 = 0$ have been presented elsewhere [5]. For that case, P rises monotically from very small values when $k_0z_1 \cos\theta$ is much less than $k_{p0}z_1$ to unity when $k_0z_1 \cos\theta$ becomes large. P passes through the value 0.5 when $k_0z_1 \cos\theta \approx k_{p0}z_1$. When $k_{p0}z_0 \neq 0$, P is small for $k_0z_1 \cos\theta$ much less than $k_{p0}z_1$ and passes through the value 0.5 when $k_0z_1 \cos\theta \approx k_{p0}z_1$; but P rises above unity and then approaches unity in an oscillatory fashion. The peak value of P increases with $k_{p0}z_0$ and the peak location approaches $k_0z_1 \cos\theta = k_{p0}z_1$ as $k_{p0}z_0$ is increased. One would conclude from the curves that the curve shape is determined primarily by the value of $k_{p0}z_0$, while $k_{p0}z_1$ determines the location of the curve with respect to the $k_0z_1 \cos\theta$ axis.

The focusing and attenuation caused by the plasma layer are apparent from the curves; the overshoot which occurs when $k_{p0}z_0 > 0$ is caused by the presence of complex poles of $Q(k_0 \sin\theta, \infty)$. Whether the poles are of leaky-wave or complex-spectral type depends upon the value of k_0z_1.

K. F. Casey
Dep. Elec. Eng.
Kansas State Univ.
Manhattan, Kan. 66502

References

[1] G. E. Stewart, "Laboratory simulation of reentry plasma sheaths," *IEEE Trans. Antennas Propagat.* (Commun.), vol. AP-15, Nov. 1967, pp. 831–832.
[2] C. T. Swift, "Radiation patterns of a slotted-cylinder antenna in the presence of an inhomogeneous lossy plasma," *IEEE Trans. Antennas Propagat.*, vol. AP-12, Nov. 1964, pp. 728–738.
[3] G. E. Stewart and K. E. Golden, "Admittance, isolation, and radiation patterns of rectangular slot antennas in the presence of a simulated reentry sheath," *1969 G-AP Int. Symp. Dig.*, pp. 215–223.
[4] M. Abramowitz and I. A. Stegun, Eds., *Handbook of Mathematical Functions* (Appl. Math. Ser. 55). Washington, D. C.: NBS, 1966, Chs. 9, 10.
[5] K. F. Casey, "Radiation through an inhomogeneous plasma covering a ground plane," *IEEE Trans. Antennas Propagat.* (Commun.), vol. AP-17, Mar. 1969, pp. 250–251.

The Upwind/Downwind Dependence of the Doppler Spectra of Radar Sea Echo

***Abstract*—A detailed investigation of the differences between the upwind and downwind Doppler spectra of the radar sea echo has been made, utilizing *P*-, *L*-, and *C*-band data obtained with the Naval Research Laboratory's Four-Frequency Radar System. The results indicate that while the Doppler bandwidth is nearly independent of wind direction, the differential Doppler looking upwind is nearly twice that for the downwind case.**

Introduction

In the intensive study of the ocean surface as a radar scatterer that has taken place during the past two decades, the major effort has been expended in the study of the ocean's radar cross section rather than on the Doppler characteristics of the radar return with the result that the physical processes affecting the noncoherent return are better understood than those underlying the coherent return. This emphasis stems, at least in part, from the fact that Doppler measurements are more difficult than power measurements and require a far more sophisticated radar system. Because of these difficulties, Doppler data have not been available in either sufficient quantity or quality to allow a comprehensive study of the Doppler return. In this respect, the Naval Research Laboratory (NRL) has made a major contribution with the Four-Frequency Radar (4FR) System which is capable of making nearly simultaneous measurements of both the coherent and noncoherent radar return over a frequency range spanning from UHF to *X* band, for horizontal and vertical polarization. Data collected with the 4FR system in the North Atlantic during February 1969, and near Puerto Rico during July 1967, were analyzed by Valenzuela and Laing [1] for wind and sea conditions that ranged from calm to 8-m waves with winds of 24 m/s. A model based on hydrodynamic principles was developed in that earlier study which predicts the wave height dependency of the Doppler bandwidth, but cannot explain the polarization dependency found in the data.

In the present study, data from the North Atlantic, along with new data collected in the relatively calm waters near Bermuda during January 1970, were used to investigate in detail the upwind/downwind dependence of both the width of the Doppler spectrum and the difference in mean frequency between horizontally and vertically polarized spectra (differential Doppler) of the radar sea echo. The results of this investigation indicate that the upwind/downwind ratio for the bandwidth is nearly unity, while that of the differential Doppler is nearly two to one. These results, along with data collected in low-wind high-sea conditions, indicate that the differential Doppler is primarily dependent on the wind speed, but that the spectral bandwidth depends on wave height.

Data Collection and Processing

The NRL 4FR system has already been described in detail in [2] and therefore, only a brief summary of its characteristics will be given. The system is an airborne, coherent, pulsed radar that uses both frequency and polarization diversity to make near simultaneous measurements of the elements of the radar scattering matrix. Operational frequencies are 428 MHz (UHF or *P* band), 1228 MHz (*L* band), 4455 MHz (*C* band), and 8910 MHz (*X* band). The return signals are range gated, and both the power and relative phase are measured and recorded on magnetic tape in a digital format for later processing.

A small general purpose computer is used to process the data and produce power spectra by means of a fast fourier transform. Several spectra computed from consecutive time periods are then averaged on a frequency-by-frequency basis to smooth statistical fluctuations. In the present study, the time periods used for analysis were approximately 1 s for *P*- and *L*-band data, and 0.25 s for *C*-band data. These time lengths yield a frequency resolution that is equivalent to the Doppler shift induced by about a 0.3 m/s change in velocity. The number of spectra to be averaged was arbitrarily chosen to be 30 for *P* and *L* band, and to cover the same total time period, 120 spectra were averaged for the *C*-band case. Because of the aircraft motion, the computed spectra are not those of the intrinsic radar sea echo, but rather the result of a convolution of the radar return spectra with the platform motion spectra. For the purposes of this report, the major effect of this convolution is the shifting of the spectra so that they are centered about the Doppler frequency due to aircraft motion.

In order to facilitate the comparison of different spectra, the frequency axis is transformed to the equivalent Doppler velocity by means of the well-known relation

$$f_d = (2v/\lambda) \cos\gamma \tag{1}$$

where f_d is the Doppler frequency, v is the magnitude of the velocity vector of the moving platform relative to the scatterer, λ is the wavelength, and γ is the angle between the platform motion vector and the direction of the propagating ray to the scatterer. Since the data included in this report is for the along-track-looking mode, γ may be taken to be the antenna depression angle, and the $\cos\gamma$ dependency, which is usually ignored, was explicitly included in the transform when working with the differential Doppler so that the internal consistency of the data could be monitored. However, the $\cos\gamma$ dependency was ignored when dealing with the spectral bandwidth.

Since the true aircraft velocity is not usually known, and the velocity of the transformed axis includes both the aircraft and scatterer motion, the true velocity of the radar scatterers cannot be found. However, the measurements made for the different polarizations are made nearly simultaneously so that the aircraft velocity should be the same for both. It is, therefore, possible to

Manuscript received December 21, 1970; revised March 1, 1971.